Electrochemical behavior of ionic and metallic zirconium in ionic liquids

Muhammad Adeel Ashraf[1,2], Markus Valtiner[1,2],
Aleksandra Gavrilovic-Wohlmuther[3], Juliane Kampichler[3] and
Christian M. Pichler[1,2]*

[1]Centre for Electrochemical and Surface Technology, Wiener Neustadt, Austria, [2]Institute of Applied Physics, Vienna University of Technology, Vienna, Austria, [3]Schoeller-Bleckmann Nitec GmbH, Ternitz, Austria

Metallic zirconium has a broad range of potential applications in engineering and in industries that are operating under harsh corrosive environments, such as nuclear and chemical industry. Compared to other metals like aluminum, its behavior in electrochemical reactions is poorly understood and so far, there are no larger-scale electrochemical approaches to process zirconium. Ionic liquids are a suitable reaction medium for electrochemical reactions of zirconium. To better understand the electrochemical reactivity of zirconium, different combinations of ionic liquids and zirconium precursors are investigated. It was found that interactions between the Zr precursor and the ionic liquids can have significant influence on the diffusion properties of Zr. Furthermore, mixtures of ionic liquids with other solvents were explored and it could be determined that most of the electrochemical properties of Zr are retained also in solvent mixtures. This could potentially save costs for industrial applications, as lower amounts of the ionic liquids can be used, to obtain similar electrochemical properties.

KEYWORDS

ionic liquids, metal deposition, zirconium, electrochemistry, metal layers

1 Introduction

Zirconium has many desirable properties such as good corrosion resistance, mechanical and thermal stability, and a low capture cross section for thermal neutrons. This makes zirconium a widely used metal in the field of nuclear technology and it is used in the metallic fuel for nuclear reactors, where it is alloyed with radioactive elements such as uranium and plutonium (Carmack et al., 2009). Zirconium concentrations of up to 10 wt% are common in those alloys. A great challenge is the recycling of the spent nuclear fuel and several approaches have been investigated to separate the alloys into its constituent metals. Electrochemical approaches are especially attractive, as they allow a straightforward separation of the main components U, Pu and Zr (Murakami et al., 2009; Krishna et al., 2018). The main reaction media for those electrochemical separations are salt melts based on KCl and LiCl,

or on KF and LiF that require high operating temperatures of at least 773 K (Xu et al., 2016; Quaranta et al., 2018). Lower temperatures would be highly beneficial for the overall process and would make the electrochemical processing of those spent nuclear fuels significantly more facile. Therefore, ionic liquids based on organic cations such as the imidazolium species have been investigated for this very process. N-butyl-N-methylpyrrolidinium bis (trifluoromethylsulfonyl) imide ([BMPyr] [TFSI]) or 1-Butyl-3-methylimidazolium bis (trifluoromethylsulfonyl) imide ([BMIM] [TFSI]) have been studied as reaction media for those purposes (Krishna et al., 2016; Vacca et al., 2016). Nevertheless, understanding the electrochemical behavior of the zirconium ions under these conditions remains limited due to the low number of studies in this field. Furthermore, the reaction of main interest for the recycling of spent nuclear fuel is the controlled anodic dissolution of zirconium, to separate it from the alloy. Controlling the cathodic deposition is of minor importance for this type of application.

Understanding the cathodic deposition of zirconium can however be helpful for a great range of other applications. Due to the excellent corrosion resistance and mechanical stability of zirconium, it is used as alloy with aluminum for formation of metallic protective layers, which are relevant for applications in armament, chemical engineering, and electronics (flash lamps) (Quaranta et al., 2018). Electrochemical deposition is a widely used method to produce such protective metallic coatings. However, electrodeposited zirconium metal has not been widely investigated for such approaches, as it would be mainly deposited from high temperature salt melts, which is not a feasible approach for most of the intended applications (Simka et al., 2009; Zhang et al., 2016; Li et al., 2021). The utilization of organic solvents as reaction medium for electrochemical Zr deposition has been reported as well (Stefanov et al., 2000; Simka et al., 2014). Rigorous exclusion of water in those solvents is required to avoid hydrolysis of the common Zr-precursors such as $ZrCl_4$. Although ionic liquids would be a potentially suitable reaction media, not enough information is available to enable the controlled electrochemical deposition of stable zirconium layers. The small number of available studies investigating the electrochemical behavior of zirconium in ionic liquids, is exclusively focusing on zirconium halides as active species and in most cases only a single combination of ionic liquid and zirconium precursor is investigated (Krishna et al., 2016; Vacca et al., 2016).

In this study, we compare for the first time several zirconium compounds [$ZrCl_4$ and Zr (acac)$_2$] in different ionic liquids [(BMIM) (TFSI) and (EMIM) Cl]. By systematic variation of the reaction conditions (Zr concentration and temperature), influence on the electrochemical behavior was evaluated. This allowed to gain insight into the interaction of the Zr^{4+} cation and its respective counter ions. As the final aim of this study is potential industrial application, the high cost of most ionic liquids is an important factor that must be considered. Therefore, cheaper Dimethylsulfoxide (DMSO) was added to the reaction solution, in order to reduce the amount of necessary ionic liquid. The electrochemical response of these mixed systems is investigated and presented in this paper. This approach can make the industrial application of metal deposition from ionic liquids, economically more feasible. Finally, the electrochemical deposition of Zr on steel substrates was tested.

2 Materials and methods

2.1 Chemicals

1-Butyl-3-methylimidazolium bis(trifluoromethylsulfonyl) imide [BMIM][TFSI] (99%),1-Ethyl-3-methylimidazolium acetate [EMIM][OAc] (99%), 1-Butyl-3-methylimidazolium trifluoromethanesulfonate [BMIM][OTf] (99%) and 1-Butyl-1-methylpyrrolidinium bis(trifluoromethylsulfonyl)imide [BPyr] [TFSI] (99%) was obtained from Proionic and 1-Ethyl-3-methylimidazoliumchlorid [EMIM]Cl (99%) was obtained from Iolitec. ZrCl$_4$ (99.5%), Zirconium (IV)acetylacetonate (Zr (acac)$_2$) (99%) and DMSO (99 + %) were obtained from Alfa Aesar. Stainless steel samples were provided from Schoeller-Bleckmann Nitec. All chemicals and materials were used as received.

2.2 Experimental setup

Electrochemical tests were performed with a Biologic SP-240 potentiostat, with a three-electrode setup, using stainless steel as a working electrode (2 cm^2), glassy carbon (2.5 cm^2) as a counter electrode and a Pd-wire as pseudo-reference electrode.

Electron microscopy was performed with a Zeiss Sigma EDVP scanning electron microscope (SEM), equipped with an Ametek EDAX analyzer for energy dispersive X-ray spectroscopy (EDX) analysis.

2.3 Experimental procedure

All experiments were performed in a glovebox under argon atmosphere (O$_2$ and H$_2$O < 2 ppm). The Zr-precursors were dissolved by magnetic stirring, at elevated temperatures in the particular ionic liquids, before performing electrochemical measurements.

Electrochemical deposition of zirconium was performed on stainless steel samples (samples were cleaned and degreased with isopropanol and dried with pressured air before utilization), at constant potential of −1.7 vs. Pd for 2 h.
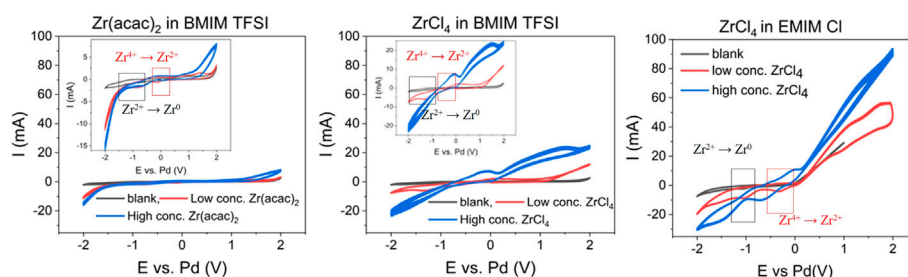
FIGURE 1
Cyclic voltammograms of: [BMIM] [TFSI] blank (black), with 0.035 M Zr (acac)$_2$ (red) with 0.12 M Zr (acac)$_2$ (blue) at 363 K (left), [BMIM] [TFSI] blank (black), 0.035 M ZrCl$_4$ (red) 0.71 M ZrCl$_4$ (blue) at 363 K (middle) and [EMIM] Cl blank (black), 0.045 M ZrCl$_4$ (red) 0.89 M ZrCl$_4$ (blue) at 363 K (right). 8 ml reaction solution; scan rate: 100 mV/s; 3-electrode setup: WE: steel (2 cm^2), CE: glassy carbon (2.5 cm^2) and RE: Pd-wire.

3 Results and discussion

3.1 Overview: Zr precursors in ionic liquids

At first, suitable reaction media have to be selected to perform the electrochemical measurements. Therefore, the chosen ionic liquid must have a suitable stability window, to allow the observation of the electrochemical features of Zr. The electrochemical stability of ionic liquids depends on their respective cation and anion combination. 1-Butyl-3-methylimidazolium bis(trifluoromethylsulfonyl) imide ([BMIM] [TFSI]) is known for its extraordinary electrochemical stability, as the [BMIM] cation and the [TFSI] anion are both stable under oxidative and reductive conditions (Ong et al., 2011). This results in an electrochemical stability window of >4.5 V. Another investigated ionic liquid is 1-Ethyl-3-methylimidazoliumchlorid [(EMIM) Cl]. The electrochemical stability window of this compound is with approximately 3 V, lower, compared to [BMIM] [TFSI]. [EMIM] Cl shows reductive decomposition of the [EMIM] cation, in a similar potential range as [BMIM], however, oxidative decomposition of the Cl$^-$ anion, is mainly responsible for the lower electrochemical stability window (ESW) (Hsiu et al., 2002; Zhang et al., 2018). As the main interest in this study lies on the cathodic deposition of metallic Zr, the lower oxidative stability of [EMIM] Cl is not considered as inhibitive. As Zr precursor, ZrCl$_4$ is selected, as it is soluble in relevant concentrations in both ionic liquids and has already proven its suitability for investigating electrochemical phenomena of Zr in ionic liquids. To better understand the influence of the Zr compound on the electrochemical behavior, Zr (acac)$_2$, was selected as well as substrate. However, it is only soluble in relevant quantities in [BMIM] [TFSI]. Other ionic liquids such as 1-Ethyl-3-methylimidazolium acetate [EMIM] [OAc], 1-Butyl-3-methylimidazolium trifluoromethanesulfonate [BMIM][OTf] and 1-Butyl-1-methylpyrrolidinium bis (trifluoromethylsulfonyl) imide [BPyr][TFSI] showed either non satisfactory solubility of the Zr precursor or insufficient

electrochemical stability. Therefore, [BMIM] [TFSI] and [EMIM] Cl were selected as ionic liquids for the further tests.

In Figure 1, the cyclic voltammograms (CV) of the blank [BMIM] [TFSI] (black traces, left, middle) and [EMIM] Cl (black trace, right) confirms the reported ESWs, with a reductive decomposition of [BMIM] and of [EMIM] at < −2 V vs. Pd. The oxidative stability is determined by the anions, with a value of 2 V vs. Pd for [TFSI] and 0.3 V vs. Pd for Cl$^-$. In the presence of low Zr concentration, clear shifts of the reduction peak can be seen. For 0.035 M Zr (acac)$_2$ in [BMIM] [TFSI], a pronounced reduction peak can be found at −0.8 V vs. Pd transitioning into a constant reductive current (approx. −1.4 V), indicating the formation of metallic Zr from the Zr^{2+} intermediate. The formation of the Zr^{2+} intermediate from the Zr^{4+} starting material, is indicated by a cathodic peak at −0.15 V vs. Pd. The reverse reactions (Zr^0 to Zr^{2+} to Zr^{4+}) are indicated by peaks in the oxidative scan, at −0.3 V and 1.4 V vs. Pd. If 0.035 M ZrCl$_4$ is used, instead of Zr (acac)$_2$, also two reduction peaks are found at approx. −0.6 V and −1 V vs. Pd, before exhibiting a constant steep reduction current at −1.3 V. Also, in the oxidation scan two peaks at 0 V and 0.2 V vs. Pd are found, followed by a large oxidative current at 0.8 V, that can be assigned to the Cl$^-$ oxidation. The different values for the particular peaks, suggest that the anions, have an important influence on the Zr^{4+} → Zr^0 reaction network. It can be expected that the hard Lewis acid Zr^{4+} exhibits stronger interactions with the small and localized charge of the Cl$^-$ anion. The (acac)$^{2-}$ anion however, with its delocalized charge seems to have weaker interactions with the Zr^{4+} cation. Hence the Zr reduction peaks appear earlier in the cathodic scan for the Zr (acac)$_2$ substrate, compared to ZrCl$_4$ [−0.15 V (Zr^{4+} to Zr^{2+}) and −0.8 V (Zr^{2+} to Zr^0) for Zr (acac)$_2$ vs. −0.6 V (Zr^{4+} to Zr^{2+}) and −1 V (Zr^{2+} to Zr^0) for ZrCl$_4$]. Additionally, the constant reductive current from −1.4 V on is more pronounced for the Zr (acac)$_2$ species, indicating that the formation of Zr^0 is proceeding more abrupt compared to ZrCl$_4$. The exact values for the reduction and oxidation peaks,

might differ comparted to the values reported in literature, as in this study stainless steel is used as working electrode, while in literature mainly carbon electrodes are utilized.

For [EMIM] Cl as reaction medium, cyclic voltammetry could be only performed with $ZrCl_4$, as Zr $(acac)_2$ is not sufficiently soluble in [EMIM] Cl. For 0.045 M $ZrCl_4$ present, the Zr^{4+} to Zr^{2+} reduction peak appears at −0.4 V vs. Pd, while the Zr^{2+} to Zr^0 peak can be found at −1 V vs. Pd. The shape of the reductive scan in the CV is similar compared to $ZrCl_4$ in [BMIM] [TFSI], indicating a similar reductive behavior of $ZrCl_4$ in both ionic liquids. The oxidative behavior is changed, as the oxidation peak is dominated by the Cl^- oxidation, which is more pronounced in the [EMIM] Cl solution due to the high concentration of Cl^- ions present.

When the concentration of the Zr precursors is increased (blue curves in Figure 1), the corresponding CV shapes change. The most obvious change with increasing of Zr concentration, is the increase in maximum reductive current at −2 V vs. Pd (−11 to −16 mA for Zr $(acac)_2$ in [BMIM] [TFSI], −8 to −21 mA for $ZrCl_4$ in [BMIM] [TFSI] and −20 to −25 mA $ZrCl_4$ for in [EMIM] Cl). This is a clear indication that the reductive current is caused by the reduction of the ionic Zr species to metallic Zr. The relatively small current increase for Zr $(acac)_2$ in [BMIM] [TFSI] in comparison with the $ZrCl_4$ substrate, is because of the larger Zr concentration of $ZrCl_4$ compared to Zr $(acac)_2$, in the high concentration tests. The concentration of Zr $(acac)_2$ could not be increased to the same level as $ZrCl_4$, due to solubility limitations of Zr $(acac)_2$ in [BMIM] [TFSI]. At concentrations >0.15 M, Zr $(acac)_2$ does only dissolve at temperatures >373°K. The solubility limit at these temperatures is approx. 0.3 M.

There is also a distinct difference in the oxidative currents. Which is lowest for the Zr $(acac)_2$ in [BMIM] [TFSI] and highest for $ZrCl_4$ in [EMIM] Cl. The high oxidative current is caused by oxidation of the Cl^- species, from the ionic liquid itself, in [EMIM] Cl or from the $ZrCl_4$ precursor. This can be seen when comparing Zr $(acac)_2$ with $ZrCl_4$ in [BMIM] [TFSI]. The system with $ZrCl_4$ shows higher oxidative currents, that further increase when the concentration of $ZrCl_4$ rises. This also means, that Cl_2 will be present in the system as reaction product of the anodic reaction, especially for longer term electrochemical processes. This might be prohibitive for various industrial applications, where Cl_2 can be detrimental for the respective application. (Haerens et al., 2009; Pradhan and Reddy, 2009).

Except for Zr $(acac)_2$ in [BMIM] [TFSI], shifts and changes of the particular reduction and oxidation peaks are found for the high concentration experiments. Peak shifts and merges are common in systems with comparably high substrate concentration, as the single peaks often cannot be resolved anymore, due to the high substrate concentration. For $ZrCl_4$ in [BMIM] [TFSI], the sequential reaction $Zr^{4+} \rightarrow Zr^{2+} \rightarrow Zr^0$ is not visible anymore. Instead, an intensive and constant reductive current commences at a potential of −1 V vs. Pd. Also, for $ZrCl_4$

in [EMIM] Cl, the steep cathodic current is shifted to −1 V. This indicates that for efficient deposition of metallic Zr, a higher concentration of Zr precursor might be helpful, as relevant amount of deposition starts already at less negative potentials. In a less distinctive manner, this can also be seen for the Zr $(acac)_2$ in [BMIM] [TFSI] system.

3.2 Diffusion behavior

A decisive criterion for the electrochemical deposition of Zr, is its diffusion behavior in the ionic liquids. Fast diffusion to the electrode surface can increase the deposition rate. The potential difference between the reductive and oxidative peak for the Zr^{2+}—Zr^{4+} redox couple is significantly larger than 33 mV for all systems (650 mV for Zr $(acac)_2$ in [BMIM] [TFSI], 500 mV for $ZrCl_4$ in [BMIM] [TFSI] and 400 mV for $ZrCl_4$ in [EMIM] Cl). This indicates that the reaction is quasi-reversible or irreversible. Therefore, the reaction is controlled by diffusion, as well as charge transfer. To probe the influence of the diffusion part, scan rate variation in CV has proven to be a suitable tool. In Figure 2, the CVs at different scan rates are depicted. The inlays show the linear correlation between the square root of the scan rate and the peak current, indicating the diffusion limitation of the reaction. For all systems, the cathodic Zr^{4+} to Zr^{2+} was chosen (see arrows in Figure 2).

The Randles-Sevcik or the related Berzins-Delahay equations provide mathematical correlations between the measured peak current, scan rate and the diffusion constant. (Krishna et al., 2016; Fabian et al., 2022) In this case the Berzins-Delahay equation (Supplementary Material Eq. S1) is better suited, to account for the quasi-reversibility of the reaction, as it contains the charge transfer coefficient α, accounting for the charge transfer influence on the reaction. A charge transfer coefficient α of 0.8 has been reported for Zr in ionic liquids, which is also used for the current calculations (Krishna et al., 2016).

By applying the Berzins-Delahay equation, the diffusion constant for the Zr species can be calculated for the different reaction systems (Table 1).

Compared with previous studies, the calculated diffusion values for Zr $(acac)_2$ are in a very similar range, while the values for $ZrCl_4$ are approximately by a factor of 10 higher (Krishna et al., 2016). The comparably large difference between the diffusion constant values for Zr $(acac)_2$ and $ZrCl_4$ indicates, that the large $(acac)^{-2}$ anion is slowing down the diffusion of the Zr species as well. It can be speculated that the anions and cations are not completely dissociated but are still loosely associated. The values for $ZrCl_4$ in [BMIM] [TFSI] and [EMIM] Cl are in a similar order of magnitude. Hence, the $ZrCl_4$ derived species can diffuse at comparable speed in both ionic liquids.

Determining the diffusion constant at different temperatures, enables the calculation of the activation energy for the diffusion
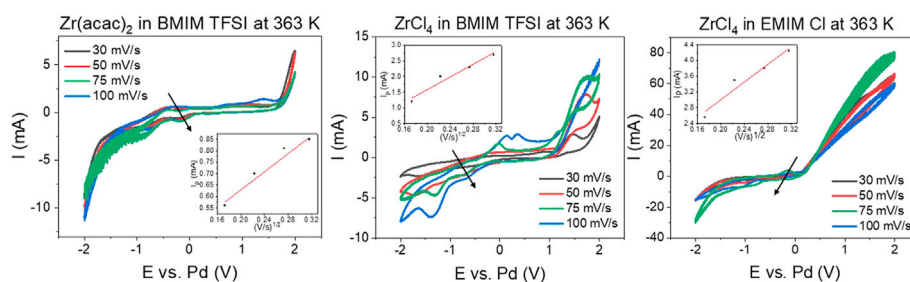
FIGURE 2
Scan rate variation for: 0.035 M Zr (acac)$_2$ in [BMIM] [TFSI] (left), 0.035 M ZrCl$_4$ in [BMIM] [TFSI] (middle) and 0.045 M ZrCl$_4$ in [EMIM] Cl (right), all at 363 K. 3-electrode setup: WE: steel (2 cm^2), CE: glassy carbon (2.5 cm^2) and RE: Pd-wire.

TABLE 1 Diffusion constants for Zr species in ionic liquids at 363 K.

Reaction system	Diffusion constant in cm^2/s $\times$ 10^9
Zr (acac)$_2$ in [BMIM] [TFSI]	2.5 ± 0.38
ZrCl$_4$ in [BMIM] [TFSI]	18.2 ± 3.4
ZrCl$_4$ in [EMIM] Cl	14.3 ± 6.1

process. Generally, it is expected that higher temperatures, lead to higher diffusion constants. In ionic liquids the viscosity of the reaction medium plays an additional important role. It has been reported that the viscosity of [BMIM] [TFSI] and [EMIM] Cl decreases with higher temperature, which also contributes to larger diffusion constants at increased temperatures (Chen et al., 2010; Nazet et al., 2015).

The Arrhenius graphs in Figure 3, enable the determination of the activation energy for the Zr diffusion process in [BMIM] [TFSI] and [EMIM] Cl. As temperature points 323, 343, 363, and 393 K were chosen. It must be mentioned that [EMIM] Cl is not completely liquid at 323 K but has a gel-like appearance. Nevertheless, we deliberately wanted to probe the diffusion behavior at these lower temperatures, as for industrial processes lower temperatures are more favorable and require less energy. Corresponding CVs for the reaction systems at different temperatures, to determine the diffusion constants are shown in Supplementary Figure S1 (Supplementary Material S1).

The activation energy E$_a$, for the diffusion process can be easily obtained from the slope of the Arrhenius graphs following the Arrhenius equation (Supplementary Material Eq. S2). The values of 0.5 KJ/mol for Zr in [BMIM] [TFSI] and 1.5 KJ/mol in [EMIM] Cl, are in the same order of magnitude, as previously reported values (Krishna et al., 2016). Nevertheless, the lower activation energy for the [BMIM] [TFSI] system indicates that the diffusion of the Zr is facilitated in this system. It can be assumed that the Zr^{4+} has a stronger affinity to the smaller Cl$^-$ ion, compared to the larger [TFSI] anion with rather soft Lewis basic characteristics. The weaker interactions with the [TFSI] anion in the [BMIM] [TFSI] reaction media, facilitate the movement of the Zr species, which is represented by the
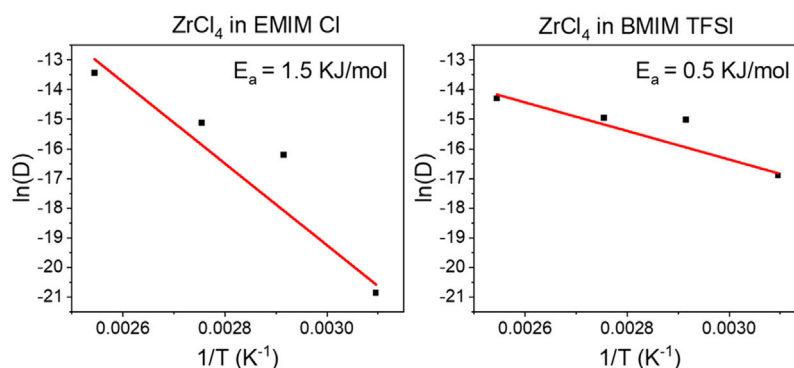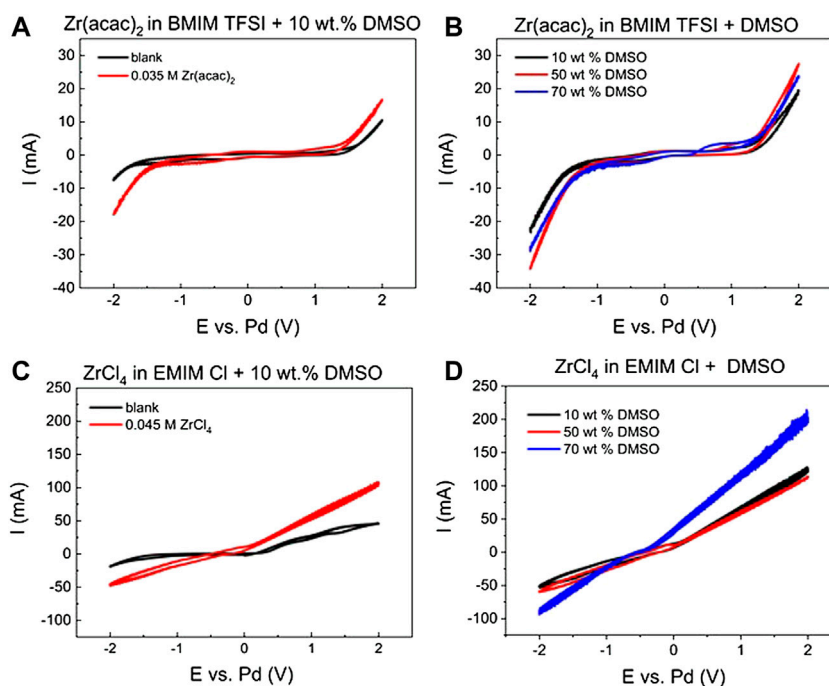

FIGURE 3
Arrhenius plots, ln(D) vs. 1/T, for 0.035 M ZrCl$_4$ in [BMIM] [TFSI] (left) and 0.045 M ZrCl$_4$ in [EMIM] Cl (right).

FIGURE 4
Cyclic voltammograms of **(A)** [BMIM] [TFSI] + 10 wt% DMSO blank (black), with 0.035 M Zr (acac)$_2$ (red) at 363 K **(B)** [BMIM] [TFSI] + 10, 50 or 70 wt% DMSO with 0.035 M Zr (acac)$_2$) **(C)** [EMIM] Cl + 10 wt% DMSO blank (black), with 0.045 M ZrCl$_4$ (red) **(D)** [EMIM] Cl + 10, 50 or 70 wt% DMSO, with 0.045 M ZrCl$_4$, all at 363 K, 8 ml reaction solution, scan rate: 100 mV/s; 3-electrode setup: WE: steel (2 cm^2), CE: glassy carbon (2.5 cm^2) and RE: Pd-wire.

lower value for the activation energy. Nevertheless, as shown previously in Table 1, the diffusion constants can still reach a comparable value in both ionic liquids if the reaction temperature is high enough.

3.3 DMSO as co-solvent

The high costs of ionic liquids are often prohibitive for the larger scale industrial applications. Dilution with compatible organic solvents, is one possibility to reduce the necessary amount of ionic liquid for a certain reaction. The prerequisite for this approach is to select an organic solvent that is miscible with the respective ionic liquid, and electrochemically as well as thermally stable under the reaction conditions. Because of its inertness and high boiling point DMSO is a suitable choice, furthermore the Zr species are soluble also in DMSO. In Figure 4, CVs for the above tested reaction systems are shown with different amounts of DMSO added.

DMSO has a comparably broad electrochemical stability window of approx. 4 V. This is demonstrated for solution with 10 wt% DMSO in [BMIM] [TFSI] in Figure 4A (black curve). Cathodic decomposition starts at approx. −2 V vs. Pd, and anodic decomposition at 1.5 V vs. Pd. If 0.035 M Zr (acac)$_2$

are added to this solution, the onset of the reductive current shifts to −1.3 V vs. Pd, as observed in pure [BMIM] [TFSI] in Figure 1. This is a strong indication that despite the presence of DMSO, Zr can still be reduced at the working electrode. Increasing the DMSO percentage from 10 to 50 and 70% (Figure 4B), leads to a shift of the onset of the cathodic reaction to −1.1 V vs. Pd. At the same time the oxidative onset is shifted to 1.3 V. This means that higher DMSO concentration causes an earlier onset of the Zr reduction, maybe facilitated by the lower viscosity of the mixed solvent reaction system. Compared to the pure [BMIM] [TFSI] system, the reaction peaks for the intermediate Zr^{4+} → Zr^{2+} reaction steps are not visible anymore. Therefore, the diffusion constants for this system cannot be determined with the Berzins-Delahay equation as previously, as no reliable peak can be selected.

If [EMIM] Cl is used in combination with DMSO, similar results are obtained. The electrochemical stability window does not shift significantly compared to pure [EMIM] Cl. With 10 wt% DMSO present, the cathodic stability limit is around −1.8 V vs. Pd and the oxidative decomposition of Cl$^-$ starts at 0.3 V vs. Pd. If ZrCl$_4$ is present, the cathodic as well as the anodic current onset is shifted in such a way that no plateau is separating the cathodic and anodic reaction part anymore in the CV. Instead, the cathodic current onset is shifted to −0.3 V, where it is already very close to the oxidation
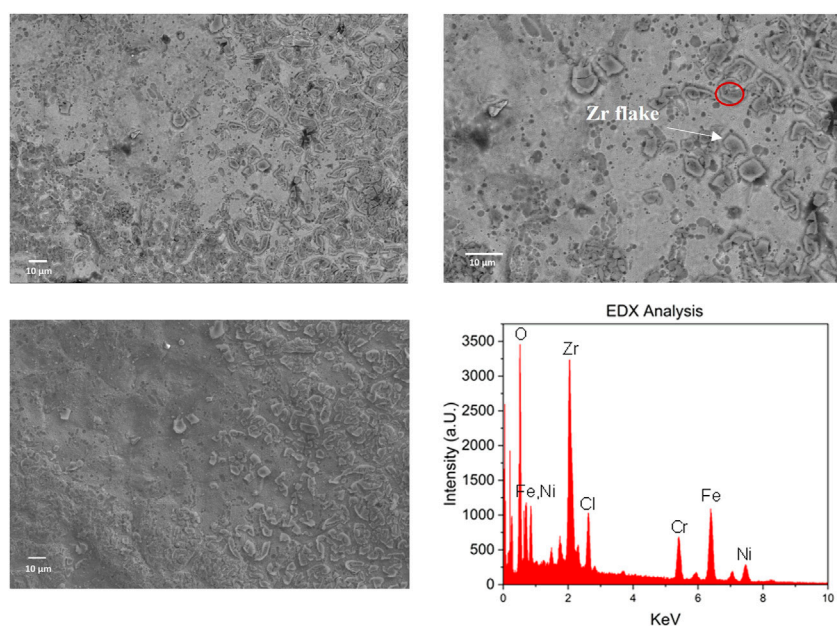
FIGURE 5
SEM images of the steel substrate after 2 h electrochemical deposition at constant −1.7 V vs. Pd in 0.035 ZrCl$_4$ in [BMIM] [TFSI], Bottom right: EDX Analysis of the marked area in SEM image (right).

current onset at + 0.3 V (Figure 4C). Similar to the [BMIM] [TFSI] + DMSO mixtures, also for the [EMIM] Cl + DMSO, distinct peaks for the Zr^{4+} to Zr^{2+} intermediate reaction steps cannot be detected anymore. If the DMSO concentration is increased to 70 wt% the slopes for the cathodic and anodic current are even further increasing (Figure 4D). Also, the peak currents at the potential maxima are, with −90 and 200 mA, significantly higher than for ZrCl$_4$ in pure [EMIM] Cl [−20 and 50 mA, Figure 1 (right)]. These results indicate that the Zr species are highly mobile in the [EMIM] Cl system and are still accessible for electrochemical reactions. The utilization of [EMIM] Cl and DMSO mixtures can be also used at lower temperatures, compared to the pure [EMIM] Cl, which has its melting point at 350 K. Therefore, the dilution of the ionic liquid can in this case even result in an increase of ion mobility. Furthermore, this is beneficial for many potential applications, as a lower reaction temperature can be used, and the amount of expensive ionic liquid is reduced.

3.4 Deposition tests

After testing the electrochemical behavior, the deposition process of metallic Zr on the steel electrode shall be investigated. Therefore, a constant potential of −1.7 V vs. Pd is applied and the potential is held for 2 h. According to the previous CV measurement, −1.7 V vs. Pd will be sufficient for the formation of metallic Zr. Afterwards, the steel substrates are investigated with SEM, to probe the surface

morphology and the chemical composition with EDX, as shown in Figure 5. Only for 0.035 M ZrCl$_4$ in [BMIM] [TFSI], the resulting Zr layers were mechanically stable. At higher concentrations of ZrCl$_4$ (<0.1 M), the reaction solution turns orange after 15–30 min. This can indicate the corrosion of the steel substrate, as iron and other elements from the steel are dissolved. The reason for this is most likely the formed Cl$_2$, derived from the anodic reaction, which has been reported previously in ionic liquids. (Haerens et al., 2009; Pradhan and Reddy, 2009) As higher ZrCl$_4$ concentrations will lead to higher Cl$_2$ production, it is plausible that the observed corrosion of the steel substrate only commences at a certain ZrCl$_4$ concentration. The corrosive environment is detrimental for the formation of a stable Zr layer on the substrate. If [EMIM] Cl is used as reaction medium, the same corrosion behavior can be observed, as the abundance of Cl$^-$ ions is now even higher. If Zr (acac)$_2$ is used as substrate in [BMIM] [TFSI], also no stable Zr layers are formed, even though no Cl$^-$ ions are present that could generate corrosive Cl$_2$. In this case it seems the interactions between the Zr (acac)$_2$ precursor, and the steel substrate are not favorable, therefore no significant nucleation of Zr can occur. Further studies are necessary, to determine the nature of the formed reaction products.

Hence, the 0.035 M ZrCl$_4$ in [BMIM] [TFSI] reaction medium, remains the only suitable medium for the formation of Zr layers on steel substrates. The SEM images of the formed Zr layers from these conditions are shown in Figure 5 and exhibit the formation of a flake-like structure on the steel surface (Zr flakes highlighted in Figure 5). EDX analysis reveals that the

flakes are most likely the deposited Zr (Supplementary Figure S2). The other elements found in the EDX spectrum such as Fe, Cr and Ni, can be attributed to the stainless-steel substrate, while Cl originates from the $ZrCl_4$ precursor. No continuous Zr layer is formed on the substrate. This is again an indication, that the interactions between the steel and the Zr are not very favorable. To obtain a continuous Zr layer, further studies are necessary to investigate the interaction of the Zr precursor and the deposited Zr with the steel surface. Key for forming a continuous and stable Zr layer, are increased attractive interactions between the Zr precursor and the steel substrate. Chemical or mechanical treatment of the steel substrate might be suitable approaches to achieve this goal, which shall be investigated in further studies.

4 Conclusion

The electrochemical studies of Zr $(acac)_2$ and $ZrCl_4$ in [BMIM] [TFSI] and [EMIM] Cl revealed that regardless of reaction medium and Zr species, the Zr reduction/oxidation proceeds in a two-step mechanism via the Zr^{2+} intermediate ($Zr^{4+} \rightarrow Zr^{2+} \rightarrow Zr^0$ and vice versa). Determination of the diffusion constants suggested that Zr $(acac)_2$ exhibits slower diffusion compared to $ZrCl_4$. This shows that the counter ion of the Zr precursor must also be considered, as it can have significant influence on the Zr mobility. When comparing [BMIM] [TFSI] and [EMIM] Cl it was shown that the activation energy for Zr diffusion is lower in the [BMIM] [TFSI] system. The reasons for this are the different interaction forces between Zr and the respective anions in the ionic liquids, however, also viscosity effects of the ionic liquids must be considered. Finally, it was shown that in mixtures of ionic liquids with DMSO, many electrochemical features of Zr are retained. This can be of high relevance for industrial applications, as the utilization of smaller amounts of ionic liquids would result in significant cost reduction, rendering hypothetical processes economically more feasible. Zr could be deposited on steel samples, at low concentrations (0.035 M) in [BMIM] [TFSI] and the resulting metal layer, had a flaky appearance. To form stable and continuous Zr metal layers on steel substrates, further investigations are necessary. In particular, better understanding of the interactions between Zr and the steel surface is required.

Data availability statement

The original contributions presented in the study are included in the article/Supplementary Material, further inquiries can be directed to the corresponding author.

Author contributions

CP and MV designed and planned the experiments. MA and CP performed the experiments and evaluated the data. AG-W and JK gave scientific input and introduced an industrial perspective on the subject. All authors contributed to writing and discussing the manuscript and agreed to the final version.

Conflict of interest

Authors AG-W and JK were employed by Schoeller-Bleckmann Nitec GmbH, Austria. This study received funding from Schoeller-Bleckmann Nitec GmbH, Austria. The funder was involved in study design and the decision to write the manuscript.

The remaining authors declare that the research was conducted in the absence of any commercial or financial relationships that could be construed as a potential conflict of interest.

Publisher's note

All claims expressed in this article are solely those of the authors and do not necessarily represent those of their affiliated organizations, or those of the publisher, the editors and the reviewers. Any product that may be evaluated in this article, or claim that may be made by its manufacturer, is not guaranteed or endorsed by the publisher.

Supplementary material

The Supplementary Material for this article can be found online at: https://www.frontiersin.org/articles/10.3389/fceng.2022.989418/full#supplementary-material

References

Carmack, W. J., Porter, D. L., Chang, Y. I., Hayes, S. L., Meyer, M. K., Burkes, D. E., et al. (2009). Metallic fuels for advanced reactors. *J. Nucl. Mater.* 392 (2), 139–150. doi:10.1016/j.jnucmat.2009.03.007

Chen, T., Chidambaram, M., Liu, Z., Smit, B., and Bell, A. T. (2010). Viscosities of the mixtures of 1-ethyl-3-methylimidazolium chloride with water, acetonitrile and glucose: A molecular dynamics simulation and experimental study. *J. Phys. Chem. B* 114 (17), 5790–5794. doi:10.1021/jp911372j

Fabian, C. P., Le, T. H., and Bond, A. M. (2022). Cyclic voltammetric experiment-simulation comparisons of the complex Zr4+ to Zr0 reduction mechanism at a molybdenum electrode in LiF-CaF2 eutectic molten salt. *J. Electrochem. Soc.* 169 (3), 036506. doi:10.1149/1945-7111/ac4b1a

Haerens, K., Matthijs, E., Binnemans, K., and van der Bruggen, B. (2009). Electrochemical decomposition of choline chloride based ionic liquid analogues. *Green Chem.* 11 (9), 1357–1365. doi:10.1039/b906318h

Hsiu, S.-I., Huang, J.-F., Sun, I.-W., Yuan, C.-H., and Shiea, J. (2002). Lewis acidity dependency of the electrochemical window of zinc chloride–1-ethyl-3-methylimidazolium chloride ionic liquids. *Electrochimica Acta* 47, 4367–4372. doi:10.1016/s0013-4686(02)00509-1

Krishna, G. M., Suneesh, A. S., Venkatesan, K. A., and Antony, M. P. (2018). Anodic dissolution of uranium and zirconium metals and electrochemical behavior of U(iv) and Zr(iv) in ionic liquid medium for metallic fuel reprocessing. *J. Electrochem. Soc.* 165 (5), C206–C212. doi:10.1149/2.0281805jes

Krishna, G. M., Suneesh, A. S., Venkatesan, K. A., and Antony, M. P. (2016). Electrochemical behavior of zirconium(IV) in 1-butyl-3-methylimidazolium bis(trifluoromethylsulfonyl) imide ionic liquid. *J. Electroanal. Chem.* 776, 120–126. doi:10.1016/j.jelechem.2016.07.015

Li, S., Che, Y., Shu, Y., He, J., Song, J., and Yang, B. (2021). Review—preparation of zirconium metal by electrolysis. *J. Electrochem. Soc.* 168 (6), 062508. doi:10.1149/1945-7111/ac0996

Murakami, T., Kato, T., Kurata, M., and Yamana, H. (2009). Electrochemical formation of uranium-zirconium alloy in LiCl-KCl melts. *J. Nucl. Mater.* 394 (2–3), 131–135. doi:10.1016/j.jnucmat.2009.08.016

Nazet, A., Sokolov, S., Sonnleitner, T., Makino, T., Kanakubo, M., and Buchner, R. (2015). Densities, viscosities, and conductivities of the imidazolium ionic liquids [emim] [Ac], [emim] [FAP], [bmim] [BETI], [bmim] [FSI], [hmim] [TFSI], and [omim] [TFSI]. *J. Chem. Eng. Data* 60 (8), 2400–2411. doi:10.1021/acs.jced.5b00285

Ong, S. P., Andreussi, O., Wu, Y., Marzari, N., and Ceder, G. (2011). Electrochemical windows of room-temperature ionic liquids from molecular dynamics and density functional theory calculations. *Chem. Mat.* 23 (11), 2979–2986. doi:10.1021/cm200679y

Pradhan, D., and Reddy, R. G. (2009). Electrochemical production of Ti-Al alloys using TiCl4-AlCl3-1-butyl-3-methyl imidazolium chloride (BmimCl) electrolytes. *Electrochimica Acta* 54 (6), 1874–1880. doi:10.1016/j.electacta.2008.10.022

Quaranta, D., Massot, L., Gibilaro, M., Mendes, E., Serp, J., and Chamelot, P. (2018). Zirconium(IV) electrochemical behavior in molten LiF-NaF. *Electrochimica Acta* 265, 586–593. doi:10.1016/j.electacta.2018.01.213

Simka, W., Majewski, D., Nawrat, G., Krząkała, A., Nieuzyła, Ł., and Michalska, J. (2014). Electrodeposition of zirconium from DMSO solution. *Archives Metallurgy Mater.* 59 (2), 565–568. doi:10.2478/amm-2014-0093

Simka, W., Puszczyk, D., and Nawrat, G. (2009). Electrodeposition of metals from non-aqueous solutions. *Electrochimica Acta* 54, 5307–5319. doi:10.1016/j.electacta.2009.04.028

Stefanov, P., Stoychev, D., Valov, I., Kakanakova-Georgieva, A., and Marinova, T. (2000). Electrochemical deposition of thin zirconia films on stainless steel 316 L. *Mater. Chem. Phys.* 65, 222–225. doi:10.1016/s0254-0584(00)00251-0

Vacca, A., Mascia, M., Mais, L., Delogu, F., Palmas, S., and Pinna, A. (2016). Electrodeposition of zirconium from 1-butyl-1-methylpyrrolidinium-bis(trifluoromethylsulfonyl)imide: Electrochemical behavior and reduction pathway. *Mater. Manuf. Process.* 31 (1), 74–80. doi:10.1080/10426914.2015.1004698

Xu, L., Xiao, Y., Xu, Q., van Sandwijk, A., Li, J., Zhao, Z., et al. (2016). Electrochemical behavior of zirconium in molten LiF-KF-ZrF4 at 600 ℃. *RSC Adv.* 6 (87), 84472–84479. doi:10.1039/c6ra17102h

Zhang, Q., Wang, Q., Zhang, S., Lu, X., and Zhang, X. (2016). Electrodeposition in ionic liquids. *ChemPhysChem* 17, 335–351. doi:10.1002/cphc.201500713

Zhang, Y., Ye, R., Henkensmeier, D., Hempelmann, R., and Chen, R. (2018). 'Water-in-ionic liquid' solutions towards wide electrochemical stability windows for aqueous rechargeable batteries. *Electrochimica Acta* 263, 47–52. doi:10.1016/j.electacta.2018.01.050